Supplementary Information

Optical virtual imaging at 50 nm lateral resolution with a white light nanoscope

Zengbo Wang[1], Wei Guo[1,2], Lin Li[1], Boris Luk' yanchuk[3], Ashfaq Khan[1], Zhu Liu[2], Zaichun Chen[3,4] & Minghui Hong[3,4]

[1]Laser Processing Research Centre, School of Mechanical, Aerospace, and Civil Engineering, University of Manchester, Manchester M13 9PL, United Kingdom.

[2]Corrosion and Protection Centre, School of Materials, University of Manchester, Manchester M13 9PL, United Kingdom.

[3]Data Storage Institute, DSI Building 5, Engineering Drive 1, Singapore, 117608, Republic of Singapore.

[4]Department of Electrical and Computer Engineering, National University of Singapore, Singapore 117576, Republic of Singapore.

Correspondence and requests for materials should be addressed to

Z.W. (email:zengbo.wang@manchester.ac.uk).

Supplementary Figures

a

b

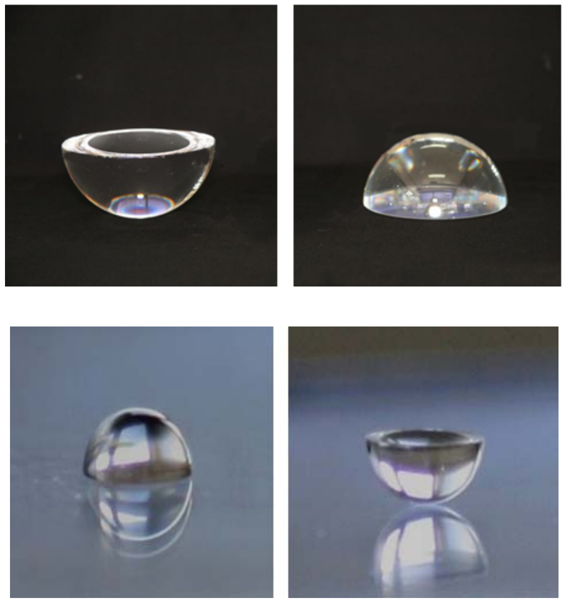

Supplementary Figure S1 | Solid Immersion Lenses (SILs) used for control experiments (**a**) 2.5 mm and (**b**) 0.5 mm. The SILs (from Edmund Optics) were placed directly onto imaging sample surface by careful manual handling, attaining an experimental configuration similar to that for the microsphere. An 80x objective lens was used for the 0.5-mm-diameter SIL and a 40x lens for the 2.5-mm-diameter SIL, as limited by the avaliable gap between lens and sample.

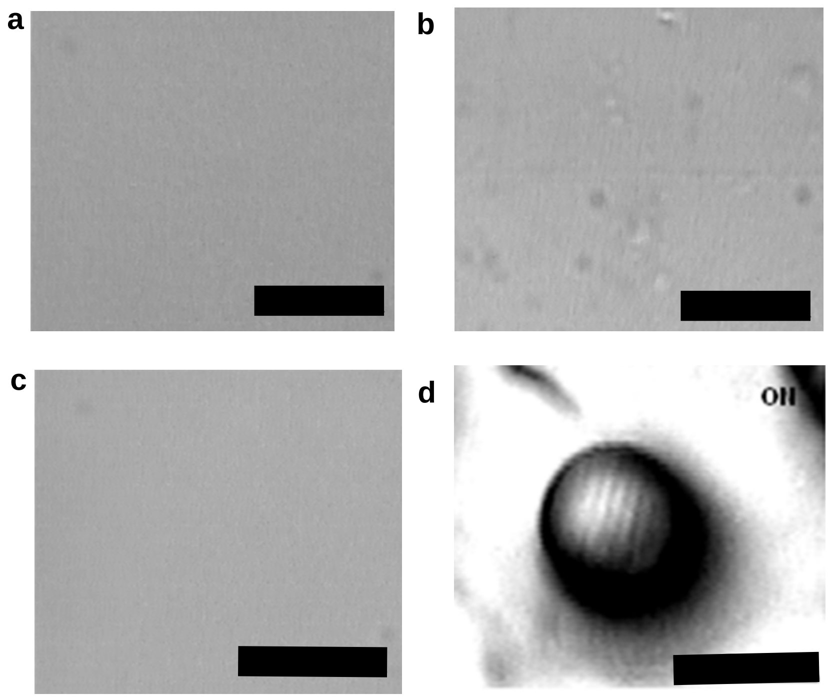

Supplementary Figure S2 | Control experiments of nano-imaging (**a**) without SILs and spheres, (**b**) with 0.5-mm SIL, (**c**) with 2.5-mm SIL and (d) 4.74- μm sphere. SILs failed in resolving underlying 100-nm-spaced line objects on the Blu-ray disk; only the 4.74-μm sphere was successful in seeing them. Similar results were observed for all other samples with feature sizes between 50 and 130 nm used in our study. It confirms that microspheres with 2 μm < diameter < 9 μm do have greater nano-imaging performance over their SILs counterparts. Scale bar, 5 μm.

a

b

c

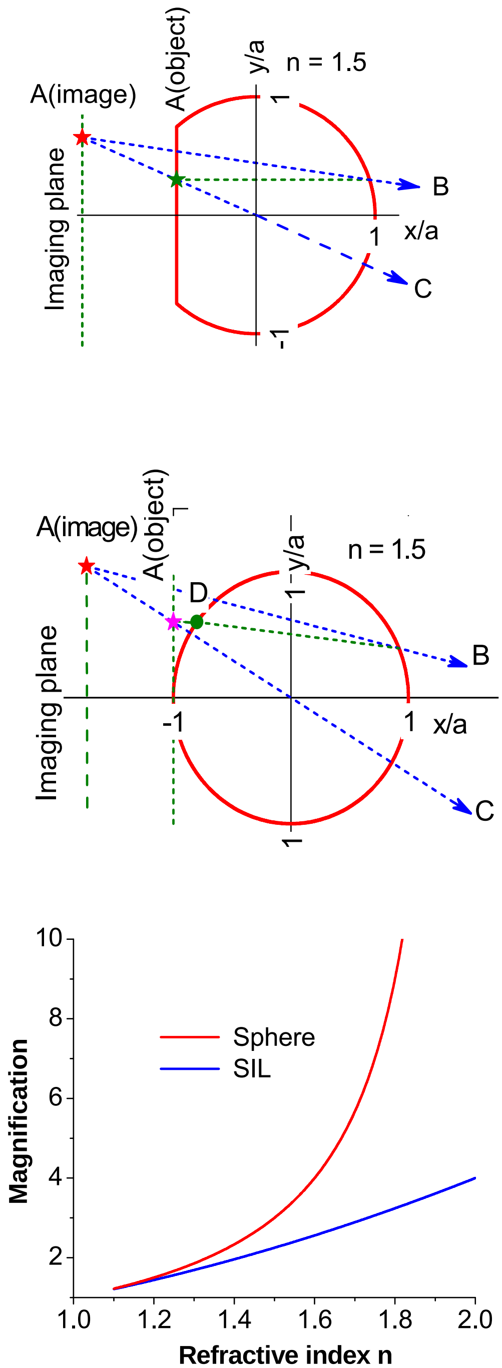

Supplementary Figure S3 | Schematic for virtual image formation by ray tracing. (**a**) solid immersion lens (**b**) spherical particle. The thickness of the SIL is $H = a\left(1+n^{-1}\right)$, where a is radius of the sphere and n is refractive index. The difference in image formation is related to refraction on the first surface, which is plane for SIL A(object) and spherical surface (point D) for the particle. (**c**) Magnification of virtual image.The spherical particle everywhere produces higher magnification than SIL.

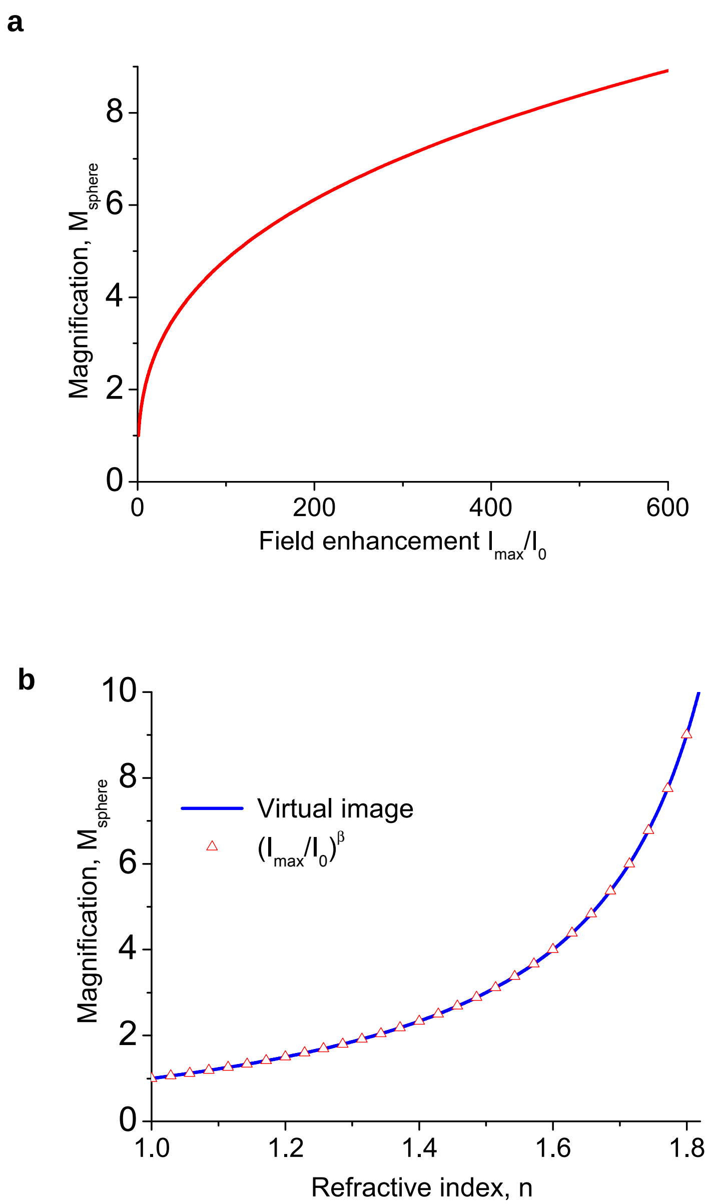

Supplementary Figure S4 | Magnification of virtual images under the approximation of geometrical optics (**a**) Magnification as a function of field enhancment. (**b**) Comparison of exact magnification of virtual image (solid line) and $M_{sphere} \approx \left(I_{\max}/I_0\right)^{\beta}$ with $\beta \approx 0.34$. Difference between the exact curve and approximated formula for $M(n)$ is less than 1% for the whole range of refractive index from 1 to 1.95. Note that geometrical optics approximation yields singularity at $n=2$, thus it cannot be applied in the vicinity of this point.

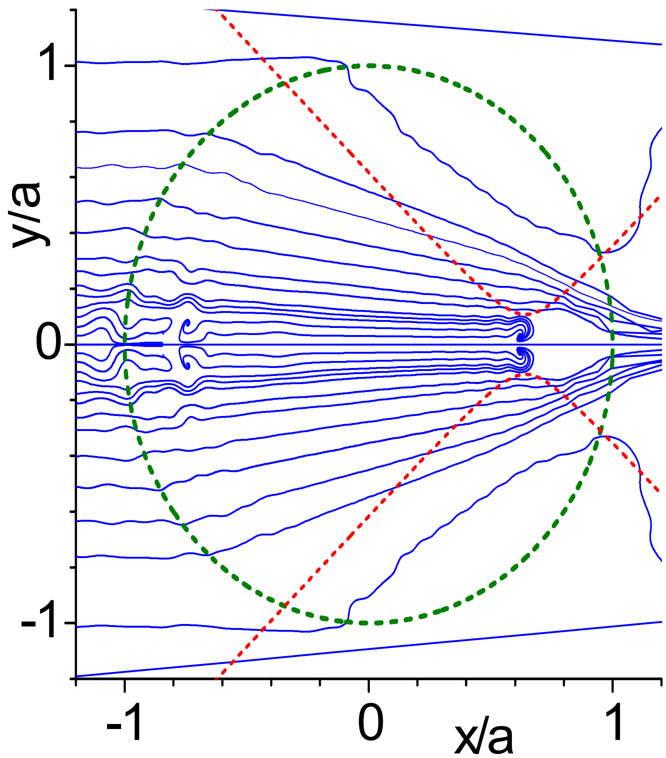

Supplementary Figure S5 | Poynting vector lines for the microsphere. The sphere radius a = 2.37 μm and refractive index n =1.46, illuminated by a plane wave with λ = 600 nm. Poynting vector lines (blue) inside the microsphere form energy vortex singularties, implying the failure of conventional geometrical optics at this size scale. Green dash lines indicate the particle. Red dot lines indicate the characteristic size of the microscope caustics.

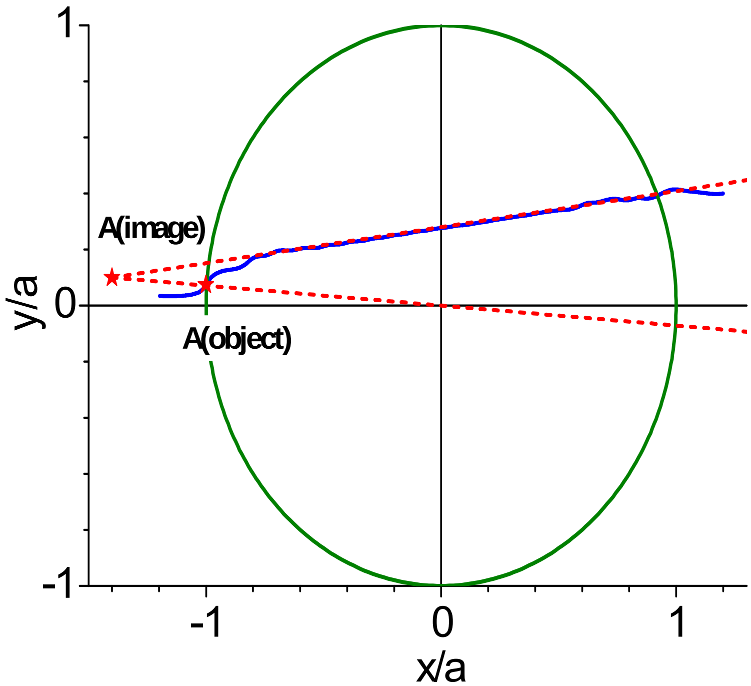

Supplementary Figure S6 | Virtual image construction in the near field. Based on the reciprocity principle, the extrapolation of the Poynting vector line could be done by plotting a tangential line to the line with some curvature, the image construction yields a magnification of 2 to 4 times depending on the particular Poynting vector line.